Bull Volcanol (1996) 58:249–262

ORIGINAL PAPER

J. D. L. White

Pre-emergent construction of a lacustrine basaltic volcano, Pahvant Butte, Utah (USA)

Received: 10 October 1995 / Accepted: 18 April 1996

Abstract The subaqueous phases of an eruption initiated approximately 85 m beneath the surface of Pleistocene Lake Bonneville produced a broad mound of tephra. A variety of distinctive lithofacies allows reconstruction of the eruptive and depositional processes active prior to emergence of the volcano above lake level. At the base of the volcano and very near inferred vent sites are fines-poor, well-bedded, broadly scoured beds of sideromelane tephra having local very low-angle cross-stratification (M1 lithofacies). These beds grade upward into lithofacies M3, which shows progressively better developed dunes and cross-stratification upsection to its uppermost exposure approximately 10 m below syneruptive lake level. Both lithofacies were emplaced largely by traction from relatively dilute sediment gravity flows generated during eruption. Intercalated lithofacies are weakly bedded tuff and breccia (M2), and nearly structureless units with coarse basal layers above strongly erosional contacts (M4). The former combines products of deposition from direct fall and moderate concentration sediment gravity flows, and the latter from progressively aggrading high-concentration sediment gravity flows. Early in the eruption subaqueous tephra jetting from phreatomagmatic explosions discontinuously fed inhomogeneous, unsteady, dilute density currents which produced the M1 lithofacies near the vent. Dunes and crossbeds which are better developed upward in M3 resulted from interaction between sediment gravity flows and surface waves triggered as the explosion-generated pressure waves and eruption jets impinged upon and occasionally breached the surface. Intermingling of (a) tephra emplaced after brief transport by tephra jets within a gaseous milieu and (b) laterally flowing tephra formed lithofacies M2 along vent margins during parts of the eruption in which episodes of continuous uprush produced localized water-exclusion zones above a vent. M4 comprises mass flow deposits formed by disruption and remobilization of mound tephra. Intermittent, explosive magma–water interactions occurred from the outset of the Pahvant eruption, with condensation, entrainment of water and lateral flow marking the transformation from eruptive to "sedimentary" processes leading to deposition of the mound lithofacies.

Key words Surtseyan volcanism · Subaqueous volcanism · Hydrovolcanism · Sediment-gravity flow · Sideromelane · Basaltic volcanism

Editorial responsibility: J. McPhie

James D. L. White
Department of Geology, University of Otago, P.O. Box 56, Dunedin, New Zealand
Fax: +64 3 479–7527
e-mail: jwhite@gandalf.otago.ac.nz

Introduction

Pahvant Butte, Utah (Fig. 1) is a volcano formed by eruption of basalt into the waters of Lake Bonneville at approximately 15300 a (Oviatt and Nash 1989). Pahvant Butte is underlain by thick deposits of Bonneville marl (muddy carbonate) deposited from the lake; earlier lavas are intercalated with lake marl at shallow levels (Gilbert 1890; Condie and Barsky 1972). The abundance of glassy basaltic particles and the distinctive volcanic morphology led to early recognition of its subaqueous origin within Lake Bonneville (Gilbert 1890). Its structure and depositional features feature prominently in a widely cited general model for tuff cone eruptions (Wohletz and Sheridan 1983), but this paper presents an alternative interpretation of Pahvant Butte eruptive processes.

Four independent lines of evidence support the contention that Pavant Butte erupted into the waters of Lake Bonneville, and was not simply reshaped by the lakewaters entirely subsequent to eruption:

1. The age of eruption has been placed reliably at between 16000 and 15300 a, during which time the surface of Lake Bonneville lay higher than the Pavant Butte eruptive site (Oviatt and Nash 1989).

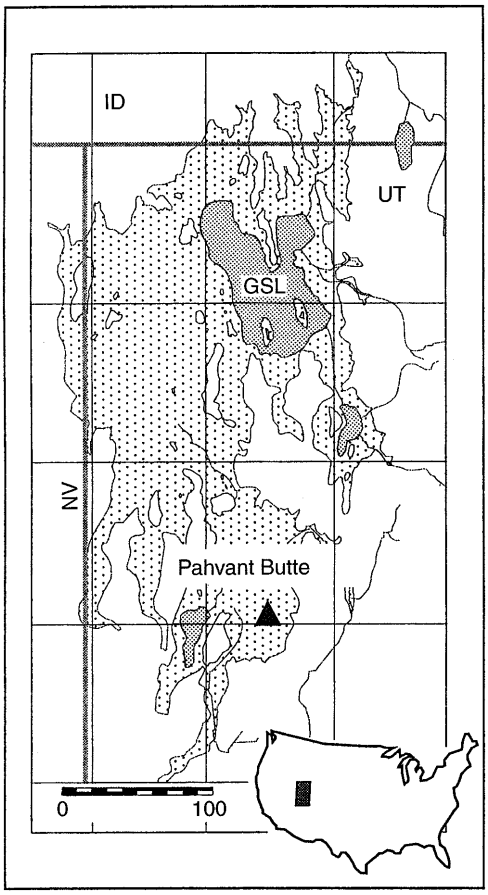

Fig. 1 Location of Pahvant Butte within boundaries of Pleistocene Lake Bonneville (*stippled*). *Broken lines* represent state boundaries of Idaho (*ID*), Nevada (*NV*) and Utah (*UT*). Scale is in kilometers. *GSL* Great Salt Lake

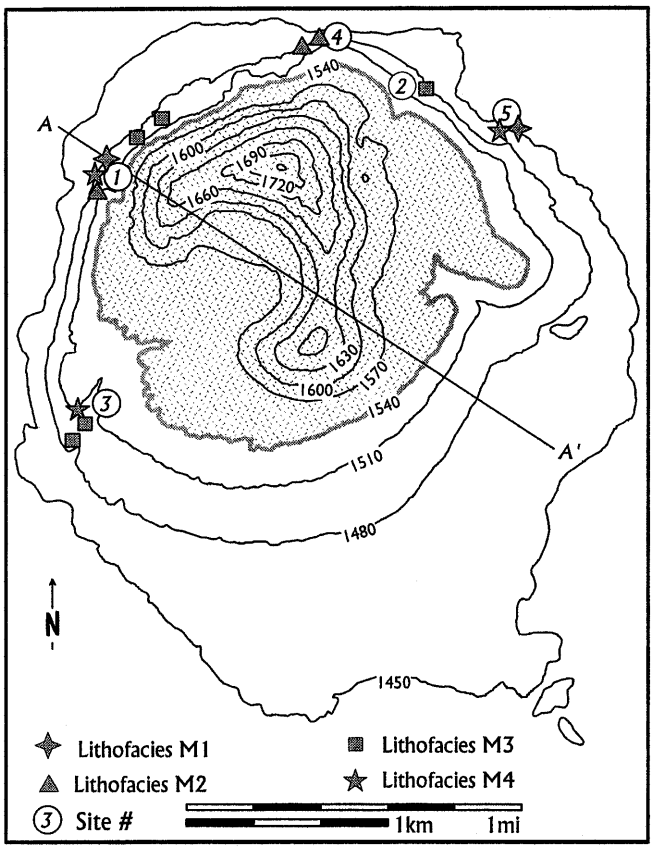

Fig. 2 Topographic map of Pahvant Butte showing locations of mound outcrops. *Thick shaded line* is syneruptive shoreline level, with subaerial deposits lightly stippled. Contour interval is approximately 30 m (100 feet). *A–A'* cross-section line for Fig. 4

2. Ash from the eruption has been identified in nearshore lagoonal marls a few meters below the widespread Bonneville shoreline (Oviatt and Nash 1989), which marks the highest level sustained by the lake (Gilbert 1890).
3. The shape of glassy pyroclasts indicates variable interaction of erupting magma with abundant water, but accidental clasts make up very little of the total material erupted. The paucity of accidental clasts suggests that hydromagmatic fragmentation was driven by surface water, rather than groundwater, because otherwise material from the aquifer would be more abundant (e.g. Fisher and Schmincke 1984)
4. Bedding features below the platform differ from those in the cone, and do not correspond to known facies of subaerial tuff cones (White and Fisher 1993).

The lower levels of Pahvant Butte preserve stratified tephra formed during subaqueous phases of the eruption. A broad mound formed during this initial stage of the eruption was subsequently modified by syneruptive erosion, and was then largely buried beneath a subaerially formed tuff cone and redeposited tephra which forms a spit/delta platform marking paleolake level (Figs. 2–4). Despite limited outcrop, the mound strata provide critical information which allows analysis of the volcanic and depositional processes characteristic of the opening stages of this explosive shallow subaqueous eruption. Early phases of the Pahvant Butte eruption produced well-bedded tephra probably from at least two vent sites, one of which lay within the upper levels of unlithified lake-floor sediments. As the eruption progressed, tephra jets began to breach the lake's surface, and bedding style changed to reflect the increased energy derived from the return of water, steam and tephra to the water after brief lofting. Lofting also engendered a more intermittent depositional style, and produced a separate early cone-forming facies nearest the vent(s). As shoaling continued deposition became localized to the subaerial cone, shoreline reworking became important (J. D. L. White, unpublished data) and mound growth largely ceased.

This paper documents lithofacies of the mound, and interprets their origin in terms of volcanic and sedimentary processes. The results are of particular relevance to analysis of other deposits from emergent volcanoes, but also have broader applications to general aspects of

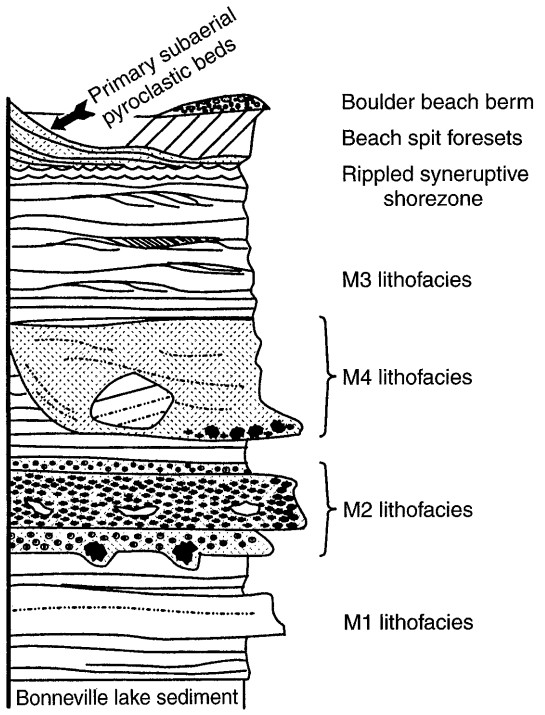

Fig. 3 Stratigraphic column of the Pahvant Butte mound deposits (unit thicknesses not to scale, but total thickness is approximately 85 m). Lithofacies association M1 is inferred to have been deposited directly on the Bonneville lake floor. It grades upward to lithofacies M3, which is characterized by dune-like bedforms and underlies syneruptive rippled shoreline deposits, which are intercalated with and overlain by primary pyroclastic beds of the tuff cone. Both primary and rippled deposits are covered by foresets of a beach-spit platform and capping bouldery beach berm. Lithofacies of M2 (near-vent deposits) and M4 (slump/debris flow deposits) are intercalated with M1 and M3 at different sites around the mound (see Figs. 2 and 4)

Fig. 4 Interpretive cross section of Pahvant Butte along line *A–A'* (Fig. 2) showing inferred architecture of mound lithofacies (no vertical exaggeration). Lithofacies M4 shown as very coarse stipple pattern, M2 in black, M3 with wavy lines above straighter lines of M1 bedding. Occurrences of M2 and M4 at different locations, at different stratigraphic heights and in association with M1 and/or M3 lithofacies indicate that vents shifted laterally and vertically with time

hydrovolcanism and eruption-fed sediment gravity flow deposition.

Mound characteristics

The mound at Pahvant Butte is covered mostly by the overlying tuff cone and by platform deposits comprising a thin upper wedge of tephra reworked in deltaic and beach-spit environments (Figs. 2 and 3). Characteristics which allow distinction of mound deposits from those of the cone and reworked-tephra platform are that all mound strata (a) have shallow dips (less than 15°), (b) are located below the syneruptive shoreline and (c) in many sites clearly underlie steeply dipping subaerial cone strata. Mound strata consist of greenish sideromelane ash grains which are weakly to moderately vesiculated and have common pyroxene and plagioclase phenocrysts, the former sometimes strongly resorbed. There is a wide range of vesiculation, consistent with phreatomagmatic disruption of a vesiculating magma (Houghton and Wilson 1989). Four lithofacies associations are defined within the mound. Deposit terminology and grain-size classification follow Schmid (1981).

Lithofacies association M1: well-bedded, broadly scoured coarse ash and lapilli

Lithofacies association M1 is exposed in cliffs and gullies not far above the level of adjacent lacustrine deposits at several sites (Figs. 2 and 5), and is inferred to have been deposited directly upon the lake floor. It consists largely of thin beds of coarse ash to fine lapilli, with minor fine ash concentrated in very thin interbeds (M1a). Bedding boundaries in M1a are subparallel, but beds show pervasive low-angle scouring, broad lenticularity and local low-angle cross-stratification, both constructional and scour-filling (Fig. 5a, b). There are rare, impersistent 10-cm-high lenses of high-angle foresets. Grain-size grading is inconsistent, with individual layers showing strong, nonuniform lateral grain-size changes (Fig. 5c). Some layers show good reverse grading at one site, changing to unsorted or normally graded at sites within distances of centimeters to tens of centimeters.

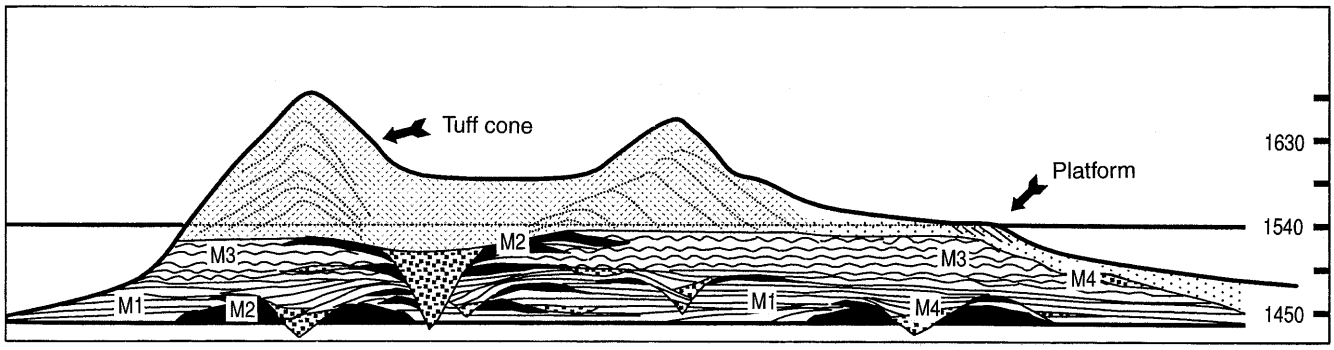

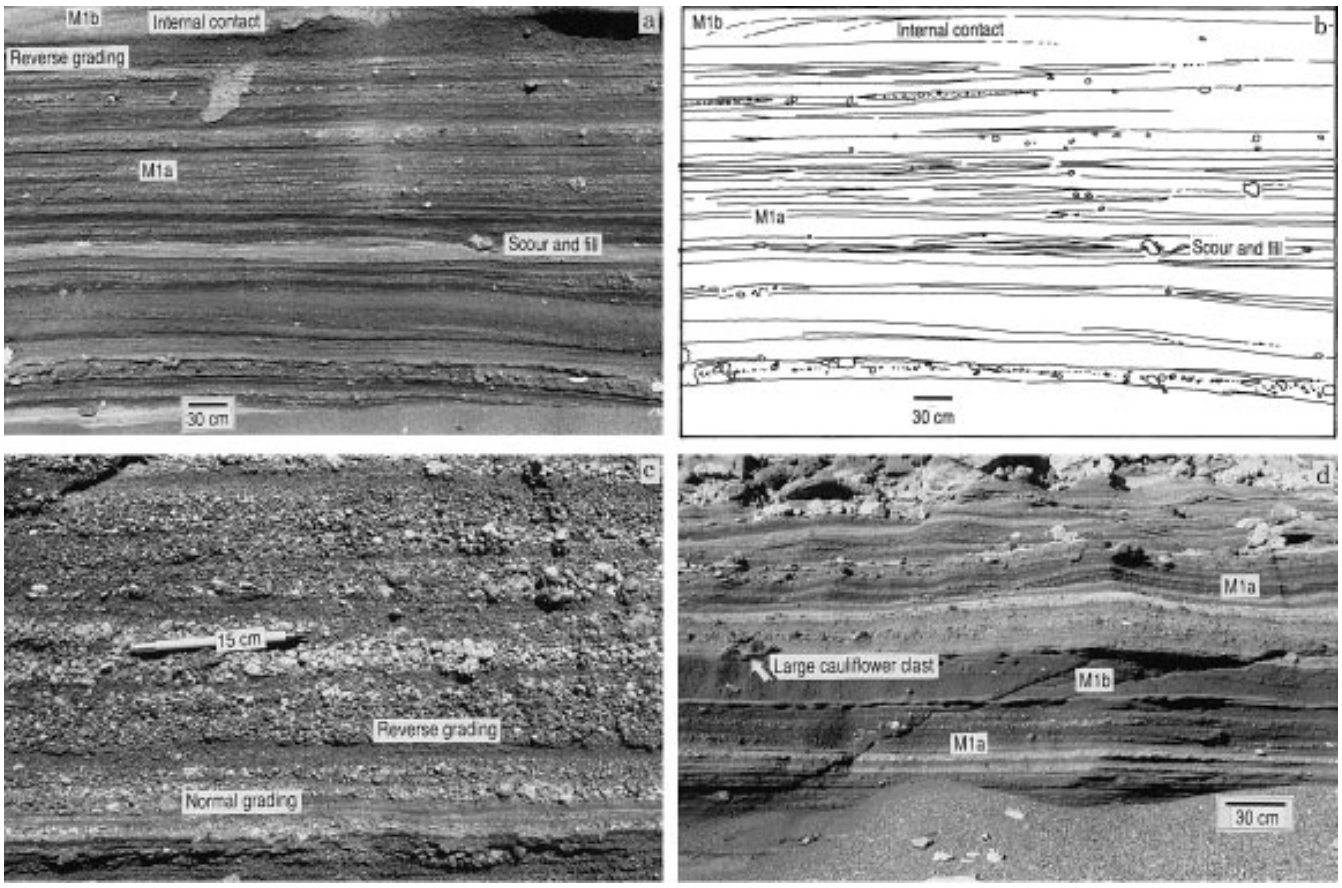

Fig. 5a–d Lithofacies association M1. **a, b** The line drawing and photograph show typical subhorizontal, very subtly lenticular bedding in the M1a lithofacies. The reverse-graded base and vague internal contacts are visible in an M1b bed near the top. Note scour and fill associated with outsize clast on right side of photo. Inferred source vent is to the right of photo. **c** Detail of M1a bedding showing low-angle scouring, normally graded layers, reverse-graded layers, cross-stratification and lateral grain-size variation in single layers (*pencil* is 15 cm long). **d** M1 tuff showing alternating horizons of dark, clean sideromelane ash and pale, carbonate-coated ash. Note absence of sags beneath larger clasts, and scour and fill to lower right of photo in M1a strata

Larger, generally cauliflower-textured, subequant clasts 5–15 cm in diameter are concentrated typically in beds of a few clasts' thickness or concentrated above the middle or at the tops of otherwise coarse ash beds. There are local concentrations of cauliflower clasts at the bases of intercalated beds of generally structureless coarse ash to lapilli beds, and many lie in clusters suggesting some degree of fragmentation during or after deposition. A few largely structureless ash and lapilli beds up to 30 cm thick (M1b) are intercalated with the thin beds (Fig. 5a, d). These thicker beds taper out laterally, and are subdivided by broad, concave-up amalgamation surfaces along which coarser clasts are locally concentrated.

A striking feature of this lithofacies association is a pronounced alternation between dark, almost black beds and pale, almost white ones (Fig. 5d). The change reflects the presence or absence of a fine-grained birefringent carbonate sediment, which partly covers grain surfaces and largely fills surface vesicles of individual clasts. The pale beds are dominated by carbonate-coated grains, and the dark ones have few or none.

Depositional processes

Broad scours, subtle bed lenticularity and very low-angle cross-stratification typify the M1 lithofacies association, yet the thin beds show good lateral continuity over tens of meters. Large clasts occur at or near the bases of beds without impact sags. Together these features suggest deposition from unchannelized, dilute, unsteady and intermittently erosive aqueous currents capable of transporting isolated large particles and depositing them together with considerably finer ones in a traction-dominated depositional regime. Although there is little fine ash, the common presence of large clasts within the medium to coarse ash beds shows that sorting overall is relatively poor, and indicates that the currents were at least at times over capacity during deposition (Hiscott 1994). Impersistent reverse-graded layers record intermittent traction-carpet deposition (Lowe 1982; Sohn and Chough 1989). The thicker, more massive beds of M1b were deposited by dense suspension from higher particle concentration flows or flow bases (Lowe 1982). The intercalation of beds com-

prising particles with and without carbonate coatings suggests derivation from two separate sources (vents).

Lithofacies association M2: massive to weakly bedded lapilli and ash with cauliflower and armored lapilli

Low cliffs at the base of the northern edge of Pahvant Butte expose intercalated coarse ash beds (M2a) and lapilli-ash breccia beds (M2b; Figs. 2 and 6). This lithofacies is of limited extent, and interfingers laterally with M1 and M3 beds. The M2a beds are of centimeter–decimeter thickness, contain a small proportion of coarse lapilli and have indistinct boundaries. Apparent size grading is limited to a weak concentration of coarse lapilli into lenses at the base of a few scour-based beds. More commonly, lapilli are concentrated in lenses, although some are isolated within ash beds. Some outsize, tachylitic, cauliflower clasts indent underlying layers, and lapilli lenses locally extend laterally from the larger clasts (Fig. 6a, b). Armored lapilli with ash coatings up to 2–3 cm thick predominate in some beds (Fig. 6a). Interbedded M2b lapilli-ash breccia is weakly bedded at a decimeter scale, with very weak normal grading of larger clasts (Fig. 6c). Most beds consist of framework-supported 3-mm/10-cm glassy, cauliflower clasts, many broken to form tight clusters of fracture-bounded fragments. Irregular clasts, many of which are deformed, of weakly altered lacustrine mudrock up to 10 cm are present. Basaltic lapilli are embedded in the bases of some large mudrock clasts, suggesting significant momentum of the mudrock clasts upon impact.

Depositional processes

Lithofacies association M2 differs from M1 in having definite sags beneath large particles, more diffuse bedding contacts, abundant armored lapilli and intercalated thick beds of coarse lapilli-ash breccia bearing many clasts of deformed lake sediment. The bedding sags suggest ballistic emplacement of the larger blocks. Lapilli lenses above the block sags indicate lateral transport and emplacement of surrounding coarse ash, as do subtle bedding deflections around blocks and local erosion. Deposition was from medium- to high-concentration sediment gravity flows into which ballistic blocks were emplaced. Lapilli lenses infilling bomb sags indicate limited traction transport during deposition. The M2a tuff beds consist largely of centimeter-scale armored lapilli, and hence must have been deposited from fairly energetic flows despite their high ash content.

Lithofacies M3: broadly cross-stratified with local steep-foreset lenses and ripples

Moderately vesicular coarse sideromelane ash with intercalated lapilli-ash and lapilli beds make up lithofacies M3, which is exposed in several locations at eleva-

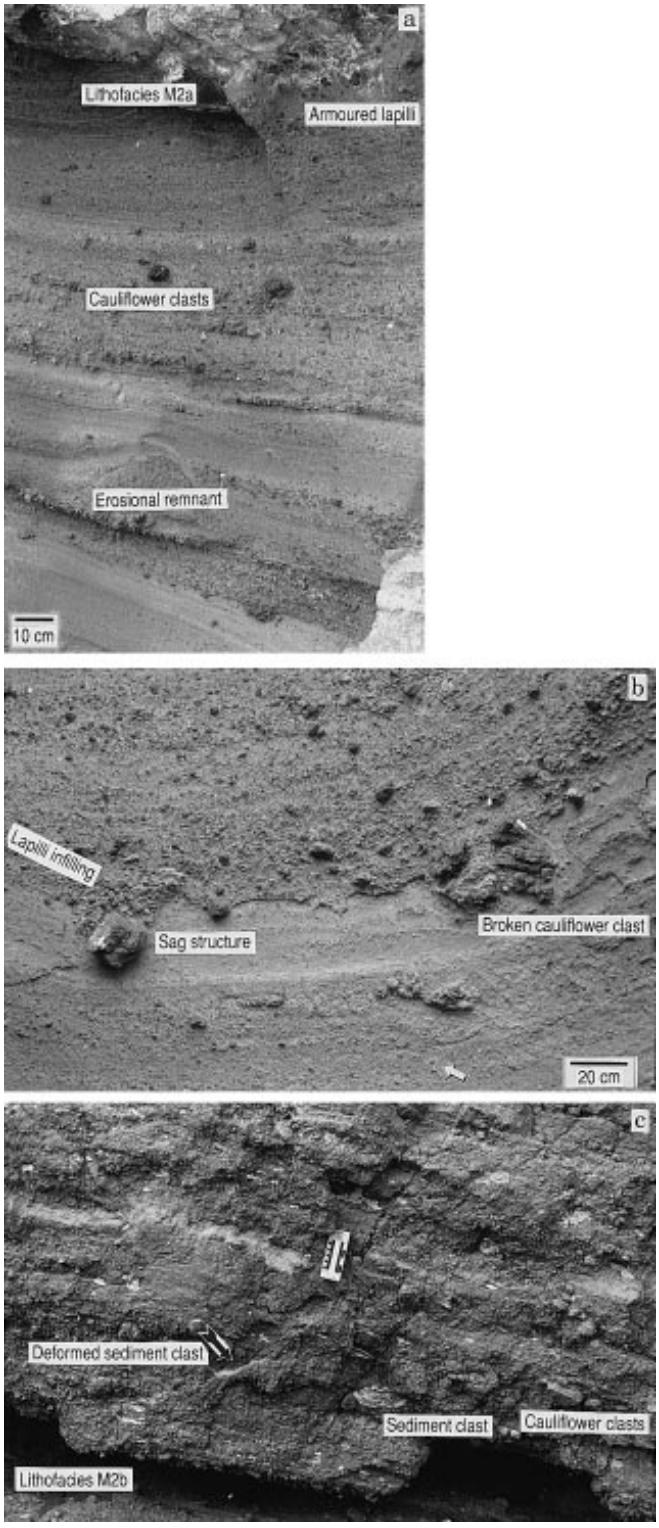

Fig. 6a–c Lithofacies M2. **a** Approximately 1-m-high outcrop of M2a ash at site-4 showing lenses of cauliflower clasts, ash-rich layers containing abundant armoured lapilli, and an eroded bed remnant with adjacent banked bedding. **b** Closeup showing abundant armoured lapilli (example *arrowed*) and sag structure in ash beneath large cauliflower clasts in M2a. Note lapilli infilling of depression above block to left. **c** M2b lapilli breccia with scattered sediment clasts, some with lightly baked margins, others strongly deformed. Note clast-supported texture and paucity of fine ash, weak layering and cauliflower-textured juvenile clasts. *Left-hand bar* on scale is 10 cm

tions slightly above M1 (Fig. 2). Where it is best exposed at site 2 (Fig. 2) it is overlain by ripple-marked shoreline beds which are in turn capped by primary subaerial tuff cone deposits (Fig. 3). The most striking depositional features of the M3 lithofacies are very broad (ca. 1 m), low amplitude (ca. 15 cm) dune-like bedforms (Fig. 7a, b). These duneforms are commonly truncated by low-relief erosion surfaces, are locally amalgamated, lack fine ash layers and have no associated sag structures. Dune bedforms have low-amplitude sigmoidal shapes where fully preserved. Locally intercalated among dune bedforms are lenses of similar coarse ash showing high-angle cross-stratification, and ripples in finer-grained ash locally advance down the gently dipping dune foresets (Fig. 7). All cross-sets have a component of dip outward from the cone, but some high-angle avalanche foresets locally dip at right angles to the main outward flow (Fig. 7c, d). The dune-like bedforms and cross-stratified lenses grade laterally and vertically into subhorizontally stratified ash layers, which are truncated by very broadly undulating erosion surfaces.

Depositional processes

The broad duneforms in coarse ash beds, high- and low-angle cross-stratification and local ripples in finer-grained ash all indicate deposition from traction at moderate velocities. Predominantly outward-dipping cross-stratification indicates transport outward from the cone. The many intercalated layers of subhorizontally layered coarse ash and lapilli ash are from suspension settling and/or lower plane bed conditions, the latter facilitated by the low density of the strongly vesiculated clasts. Cross-stratification, duneforms and ripples are best developed at higher levels, and extend to the uppermost exposures of the mound at paleodepths of approximately 20 m below syneruptive lake level. At greater paleodepths, approximately 50 m or more below lake level, facies M3 grades downward into M1.

This facies developed by interaction between aqueous sediment gravity flows and oscillatory flow beneath

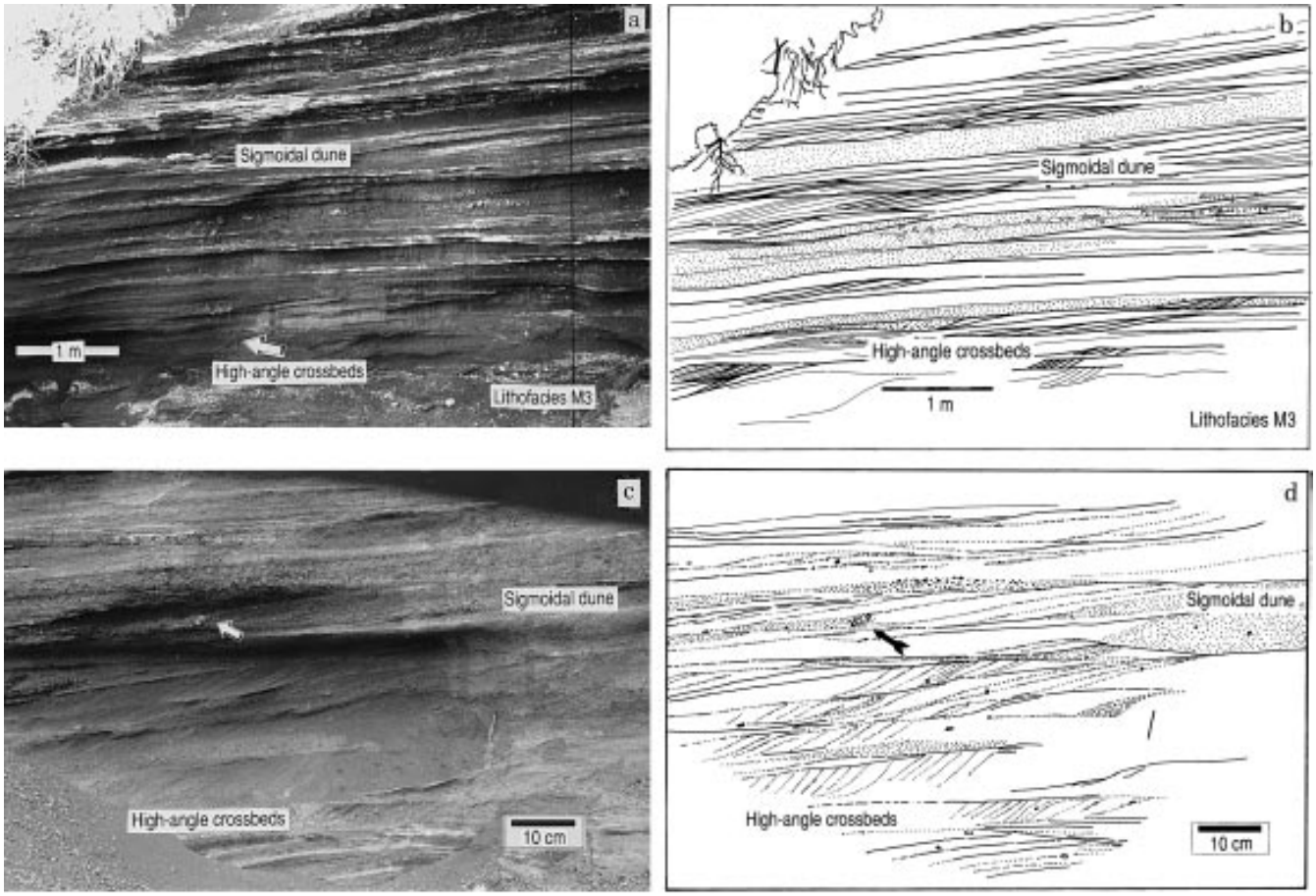

Fig. 7 Lithofacies M3. **a, b** Pervasive low-angle lenticularity and sweeping truncation surfaces typify this lithofacies (site 2, Fig. 2). Thicker massive or subtly stratified beds are *stippled* on the drawing made from the photo. *Vertical line* marks edge of area in drawing. **c, d** High- to low-angle cross-strata in M3. Note low-angle cross-stratification in sigmoidal duneforms, and concentration of lapilli at toes of gentle of cross-strata. Bedding surfaces descend gently to the left (to NNE, outward and downcurrent from cone)

surface waves. Pervasive form discordance, defined especially by smoothly undulating truncation of the tops of cross-sets, amalgamation of cross-sets and broad scours in subhorizontal layers, are typical of wave-generated sedimentary sequences (Raaf et al. 1977; Allen 1982). The similar dips of stoss and lee side layers, in combination with unidirectional internal cross-stratification, is also typical of bedforms generated from combined oscillatory and unidirectional flows (Southard 1991). These bedforms are in strata, that formed prior to emergence of the volcano, as indicated by the overlying rippled shoreline deposits and subaerial tuff cone beds. There is no intercalated lacustrine silt or mud which would indicate substantial quiescent periods during eruption. Sediment gravity flows fed directly from the vent region were responsible for the persistent outward transport. Wave-generated oscillatory currents, superimposed on the outward flows, produced the form-discordant dune-like bedforms.

The grain size of these beds is coarse compared with those of other sequences showing similar wave-generated structures (cf. Raaf et al. 1977; Allen 1982). Two factors explain this difference: One is that the particles are of relatively low density because they are vesicular. Coarse-sand-grade (–0.5 phi) vesicular pyroclasts have settling velocities equivalent to those of medium quartz sand (ca. 1 phi; Oehmig 1993). In addition, the sediment was deposited from density currents, but at depths well within wavebase. This situation does not arise normally in equilibrium shelf environments, where sandy sediment deposited in wave-generated sequences must be delivered by relatively weak storm-surge generated gradient currents (Allen 1982), or perhaps in some rare instances by turbidity currents prior to storm reworking (Fenton and Wilson 1985).

Lithofacies M4: thick bedded, faintly stratified ash with rotated tuff blocks

Thick beds of structureless to subtly stratified siderome-lane ash and lapilli-ash are observed in contact with M1 and M3 lithofacies. These beds have reversely graded margins and commonly contain rotated blocks of bedded ash. Internal contact surfaces and faint layering are apparent in most M4 tephra, and are particularly well developed in a U-shaped channel incised approximately 6 m into M1 beds at site 1 (Figs. 2 and 8). Many M4 units contain rotated blocks of bedded ash up to a few cubic meters in volume. These blocks lie within a coarse-ash tephra matrix lacking significant fines and showing modest reverse-grading near the scour margins. Elsewhere weak normal grading characterizes coarse lapilli which are concentrated at the base of M4 units especially in scours. Inclined inward-dipping layers are present locally at the lower margins of M4-filled channels, and at the edges of irregularities at the base of M4 units.

Depositional processes

Lithofacies M4 is the least characteristic of the mound lithofacies. Very similar deposits are also present in spit/deltaic foreset units of the platform and on the subaerial Pahvant Butte cone (J. D. L. White, unpublished data) and other emergent cones (Sohn and Chough 1992). The irregular, partly U-shaped bases of massive M4 units record strong erosion. Rotated blocks of bedded tephra suggest partial disaggregation and transport of earlier ash deposits (White and Busby-Spera 1987). Subtle, subhorizontal internal stratification is present generally in the M4 matrix, and may record rising depositional surfaces (Postma et al. 1983; Kneller and Branney 1995) during sedimentation from high-concentration, sublaminar flows. The inward-dipping inclined strata record lateral accretion at some channel edges, and suggest that some channels migrated laterally during deposition (Cas and Landis 1987). Preservation of the rotated blocks of still-friable bedded ash suggests essentially nonturbulent flow and very limited transport distances.

Observations on edifice emergence based on the Surtsey eruptions

The next sections (a) summarize observations of subaqueous explosive eruptive activity, (b) interpret processes of pre-emergent eruptive processes in light of the observations and (c) analyze Pahvant mound lithofacies in light of (a) and (b). Interpretation of mound depositional features is hampered by the fact that the only aspects of subaqueous eruptions which have ever been observed are those visible at the water surface, and even those only briefly and from a distance (e.g. Thorarinsson 1967). There are few published data concerning the details of subaqueous eruptive processes. Surtsey itself was first noted by fishermen, from sulphurous odours and an irregular movement of their boat. When first observed at approximately 7:30 a.m., 14 November 1963, "dark smoke" was rising into the atmosphere. The captain saw "... black eruption columns rise just above the surface of the sea..." (Thorarinsson 1967, p. 14). By 8 a.m. "... the tephra columns had reached a height of 200 feet (66 m) and rose from the sea in two or three separate places. At 10 o'clock ... the black columns ejected stones, and flashes occurred, but so far the eruption emitted no noticeable noise." (pp 14–15). A photo taken at this time (Thorarinsson 1967, plate 2) shows a large circle of whitened water, representing a zone of agitation containing vapour bubbles. This zone in the photo extends beneath and beyond the still-lofting tephra jet, and beyond the steamy, particle-poor base surges as well. Concentric waves with wavelengths greater than those of the ambient North Atlantic travel away from the vent. Water temperature was approximately 9°F warmer than normal. By 3 p.m. the sea was beginning to break on some new obstacles, and the

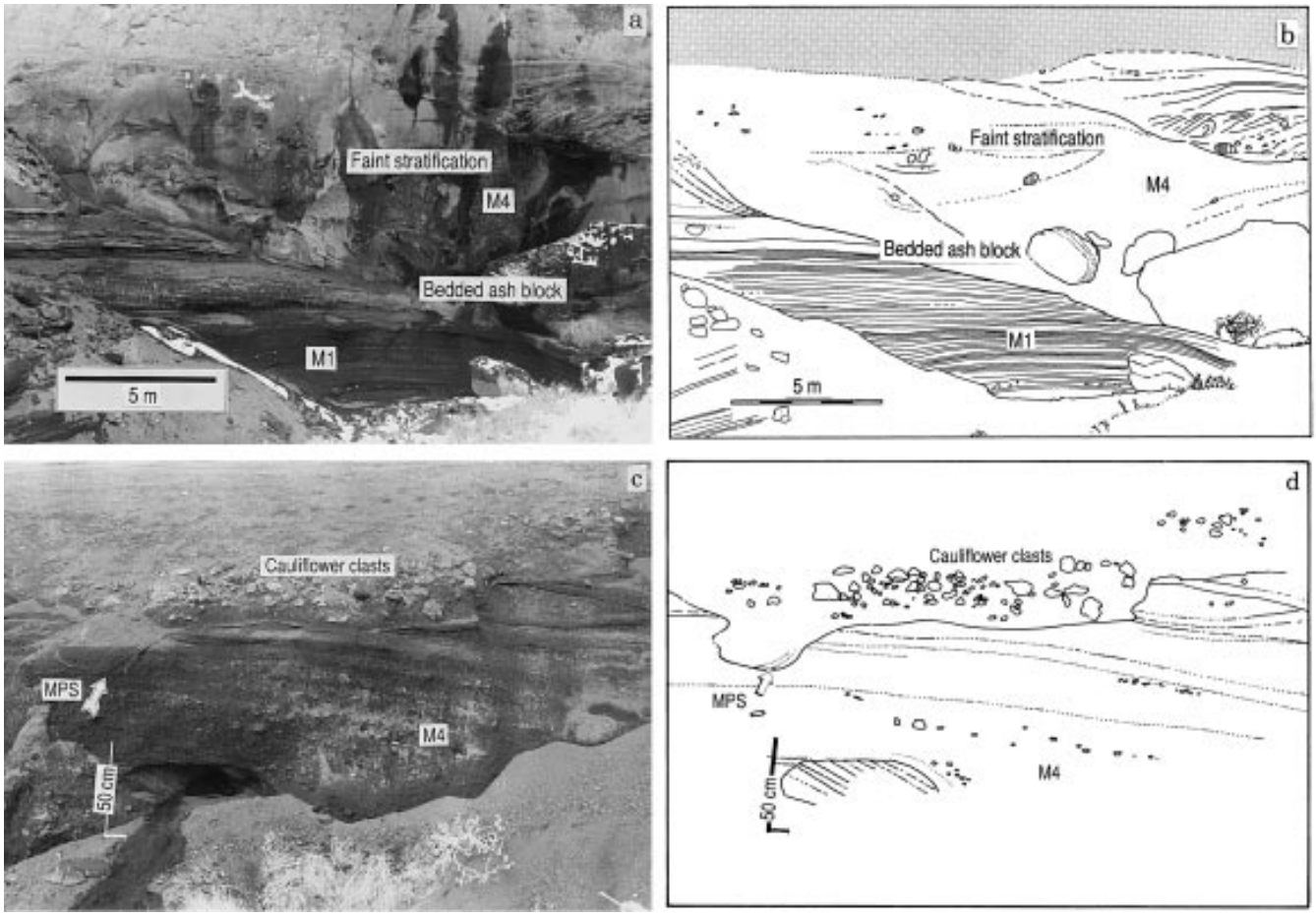

Fig. 8 Lithofacies M4. **a, b** Thick M4 unit incised into M1 ash, looking northward at site 1 (Fig. 2). Rotated blocks of weakly lithified M1 ash lie within lapilli ash which shows faint stratification dipping away from source. The base of the M4 unit has a thin layer lacking larger clasts, and a second, margin-parallel contact is weakly developed (**b**). Note the well-developed sigmoid stratal bundle climbing outward from the upper right. **c, d** M4 strata at site 3 showing, near base of outcrop, a block of rotated bedded M1 ash, just to right of scale, within M4 lapilli ash having subtle subhorizontal stratification. Note irregular base, local margin-parallel stratification (MPS) and concentration of cauliflower bombs in uppermost exposed unit (M4)

eruption was coming from a fissure approximately 1600 feet (525 m) long, with a vapour column which reached 4 miles (6.5 km). By the next morning Surtsey was emergent, 33 feet (11 m) high and in fairly constant eruption.

Three satellite vents to Surtsey were observed as they approached the surface of the sea. The first observations of the *Surtla* vent took place when the mound had closely approached the surface and eruptive activity had begun to affect the water surface. Fishermen first reported "turbulence" in the water. Steam was reported rising from the sea the next day and "... the sea showed considerable signs of unquietness." Thorarinsson (1967) reported that ".... a short way under the surface – our guess was 2 feet (0.66 m) – three small vents were active in about an 820-foot-long fissure (269 m).... When we flew very low straight above these new vents quick flashes from fire under the surface could be seen at intervals of half a second, causing abrupt concentric waves all around that made the sea look like quivering jelly. Occasionally steam columns rose above the surface, and in between there were black outbursts of tephra which ejected columns ... highest reached a height of 160 feet (52 m)." (p. 21). The first photo plate (Thorarinsson 1967) shows a tephra jet lofting material into the air, vapourous base-surge clouds, and a circular zone of agitated, whitened water (vapour bubbles) beyond the surges. The eroded remnant of Surtla, 40 m below sea level, was later found to hold abundant tachylite grains and plastically deformed clasts (Kokelaar and Durant 1983).

Initial observations of the *Syrtlingur* vent on 23 May 1965 followed sightings of occasional steam clouds rising into the atmosphere on 11–22 May (Thorarinsson 1967). There was a "brown patch in the sea" , but no steam or "unusual movement in the sea" was observed (Thorarinsson 1967, p. 32). The next day the sea "boiled" above the vent, and brownish pumice floated in the water. In the afternoon windows were rattled 10–20 km away in the Vestmann Islands, probably from explosions at the vent. By the afternoon of 24 May a

broad crater was barely visible beneath the water. On 25 May (Thorarinsson 1967, p. 34 and 34),

"explosions occurred then in this new crater at intervals averaging 15 seconds, and reeking lumps of tephra were seen to fly a few yards above the surface of the sea. In the early afternoon of May 26th there were fairly large explosions at intervals of 1–3 minutes with dark tephra columns rising about 60 feet (20 m) up in the air.... As the sea grew calmer between the explosions the rims of a circular vent, about 500 feet (164 m) in diameter, could be seen quite clearly just under the surface, with steam rising from the crater rims all round." (p. 32)

... "it was not until the early afternoon of May 28th that it was seen for the first time as a small mound in the sea.... There were no explosions then and no fires could be seen. The mound disáppeared the following day. During the next few weeks the eruption increased steadily. On June 3rd the explosions hurled solid materials to a height of 160 feet (52 m) and a column of smoke rose hundreds of yards up in the air, but fairly large patches of the sea were covered with floating pumice. It was, however, not until June 5th that an island emerged from the sea again, and in the evening of June 6th it was found to be 35 feet (11 m) high and 115 feet (38 m) in diameter.... It had the shape of a hoof with an opening towards the southeast." (p. 34)

The last of the Surtsey satellites to be seen emerging from the sea was *Jolnir*, first observed by Thorarinsson (1967) on 26 December 1965. It was issuing a continuous volume "... of steam from an area which was about 160 feet (52 m) wide ... and at 2 to 3 minute intervals black tephra columns stretched a few dozen yards up in the air ... the crater rims were just under the surface of the sea." By 4 June of 1966 Jolnir had emerged repeatedly and been washed away and "... its height was about 120 feet (39 m) and its area about 70 acres (28.3 hectares). Contrary to the Syrtlingur which was mainly a tephra cone, most of the new island is flat land and landings on its shores have involved no danger although the tephra fall is heavy at times." (p. 36)

Interpretation of Surtseyan activity prior to and during earliest stages of edifice emergence

Each of the satellite eruptions of Surtsey came to attention initially due to either steam rising into the atmosphere or turbulence in the surface waters. The latter probably represented agitation of the water surface by hot, convecting water, while steam rising above water indicated passage of vapour bubbles through the water surface. The whitened circles of water surrounding vents during explosive eruption were likely "spall domes" intersecting the surface; the circles thus represented the zones within the primary pressure waves (shock waves) generated by the explosions (Cook 1958). Slightly later, subaerial tephra jets joined with the turbulence and steam. These three phenomena can all arise from subaqueous tephra jetting, the result of explosive hydrovolcanic disruption of magma at shallow depths. Vigorous tephra jets from a vent slightly below the surface had sufficient momentum to clear the water surface. Less vigorous ones lost momentum before breaching the surface, but generated sufficient steam, as the jet collapsed and fragments directly contacted surrounding water, to feed a vapour column rising through the surface. Hot fragments continued to generate steam even after deposition, as indicated by the steaming subaqueous crater rims of Syrtlingur. Weaker, intermittent bursts agitated the water and sent heated pockets of water to roil the surface, but the steam generated from the bursts was recondensed in the cold ambient seawater before reaching the surface.

Explosive, hydrovolcanic fragmentation is indicated by the subaqueous incandescent flashes noted at Surtla, and subaqueous explosions at all vents. The subaqueous flashes are interpreted to have been caused by explosive disruption of large lumps of incandescent magma by hydrovolcanic explosions. Shock waves and outward-travelling concentric surface waves were seen at each vent during shoaling. Within the area swept by shock waves there was differential acceleration of water compared with the already-deposited tephra beds, but the differential was small because the tephra beds were water-saturated and uncompacted (Henrych 1979). Explosion-induced shaking likely caused local failure of the growing edifice, displacing variably sized parts of the mound downward along local slips (Godcheaux et al. 1992). The main effects of the shock were to agitate the water, generate vapour bubbles and initiate concentric surface waves.

Multiple vents were active at Surtsey and Surtla. Prior to emergence, broad, low-relief tephra mounds were visible near the surface. The mound surfaces accreted tephra from the varied eruptive activity and were disturbed both by normal sea waves and concentric eruption-generated waves. Wide craters, as observed at Surtla and perhaps Jolnir, would have accumulated a tephra slurry by fallback from nonbreaching jets, essentially of the type proposed by Kokelaar (1983, 1986). This "almost emergent" phase of edifice construction, in which emergent eruptive activity is commonplace, lasted for more than 2 weeks at Syrtlingur vent. If one includes the period during which emergent eruptive activity precedes *lasting* edifice emergence, the time can run to months for single vents (Syrtlingur, Jolnir, Surtsey itself) to decades or longer (Hoffmeister et al. 1929).

Extrapolating downward from this observed activity, it is expected that the influence of surface waves will decrease downward. Pressure waves resulting from hydrovolcanic explosions are probably generated effectively to depths of 100 m or more (Yamamoto et al. 1991), and thus persist to depths greater than fair-weather wavebase. These affect the movement of tephra jets into the water, but have little direct effect on

depositional processes. Tephra jets rarely pierce the surface from more than a few meters depth, and when the vent is more deeply submerged their energy is expended in heating and agitating the water above the vent. As each jet dies out in the water column, subsequent tephra dispersion and deposition take place by entirely aqueous means (Fig. 8).

The presence of tachylite grains and plastically deformed clasts suggest that direct magma–water contact was not ubiquitous during the (wholly subaqueous) Surtla eruption. Kokelaar (1983, 1986) interpreted these features to indicate development of a steam cupola during eruption which shielded much of the erupting tephra from the ambient water. Such a cupola was envisaged to form only during "continuous-uprush", high-magma-supply stages of the eruption. Unfortunately, no episodes of continuous-uprush activity were actually observed during Surtla's near emergence; thus, there is no information concerning surface (or subsurface) manifestations of the process.

Subaqueous eruption and deposition of the Pahvant Butte mound

In this section observations of Surtsey are integrated with inferred depositional processes of the Pahvant Butte mound lithofacies to interpret the mound-forming stage of the Pahvant eruption.

Eruption and deposition of lithofacies M1

The earliest stages of the Pahvant Butte eruption are represented by the M1 lithofacies association. Alkaline basaltic magma erupting in less than 100 m of water vesiculates freely, which is consistent with the moderate to strong vesicularity of the coarse ash in even the lowest M1 mound deposits, and with the absence of exposed pillow lava or recognizable pillow lava fragments anywhere at Pahvant Butte (Staudigel and Schmincke 1984; Kokelaar 1986). The M1 lithofacies association typically contains common, but not volumetrically important, chunks of lake-floor carbonate sediment and sediment-coated clasts, and was deposited in conformity with the flat pre-eruptive lake floor. Many meters of unconsolidated muddy carbonate sediment (marl) underlay the Pahvant Butte eruptive site, and the relative paucity of such sediment in the eruptive products suggests that the magma passed rapidly and efficiently to the surface. The presence of earlier lavas not far beneath the lake floor is expected to have helped stabilize the erupting vents, lessening any tendency to widen or excavate more deeply into the lake floor.

Initial eruptions did not break the water surface and produced an abundance of coarse, weakly vesicular sideromelane fragments mixed with clasts of stiffened lacustrine carbonate sediment. Interlayering of beds dominated by carbonate-coated clasts with beds containing very few such clasts suggest that separate source vents were initially active, and that one was excavated some small distance into the underlying lake sediments, becoming filled with a recurrently ejected slurry of sideromelane and carbonate sediment. Sharp contacts between the two bed types are difficult to reconcile with intermittent magma-sediment mixing in a single vent, because the vent would not be cleared fully by each discharge (Kokelaar 1983). Assuming that shallow subsurface conditions were fairly homogeneous beneath Pahvant Butte, retreat of one of the vents downward into the sediment may suggest lessened extrusion rates at that vent, whereas the black beds represent clear vent, generous discharge conditions (for M1 beds). Steam-rich tephra jets carrying quenched pyroclasts shot into the water behind the pressure waves generated by hydrovolcanic explosions, collapsing as their steam condensed and releasing particles which fell back toward the vent (Figs 9 and 10a). Semicontinuous jetting from the vents, however, generally diverted the dense fallout to feed outward flowing ring-shaped currents of tephra-laden water. These currents were unsteady and turbulent, with strong fluctuations in density and temperature and local pockets of steam around hot clasts. M1a was deposited from bedload at the base of these unsteady aqueous currents; deposition alternated with erosion by turbulent cells in the currents. Relatively low sedimentation rates within the currents are suggested by the paucity of fine ash (Lowe 1988; Hiscott 1994). During brief pauses in activity tephra accumulated to form a slurry in the upper vent. Subsequent jets displaced the slurry from the vent, and it flowed outward in high-concentration flows to form the relatively thick, structureless M1b beds. The M1 deposits constructed a gently sloping mound which built up from the lake floor and extended beyond the vent(s), and which further enhanced the mobility of flowing material in the pyroclast-rich currents.

Eruption and deposition of lithofacies M2

Features indicative of ballistic, gas-phase transport typify this lithofacies, particularly the heavily armored lapilli, abundant bomb sags and tachylitic larger clasts. Preservation of accretionary clasts in subaqueous environments is now well established (e.g. Dimroth and Yamagishi 1987; Ballance and Tappin 1993; McPhie et al. 1993). Subaqueous formation of such clasts has not been demonstrated, but should be possible, particularly if formation of armored lapilli took place in several stages by repeated circulation of the clasts in a vent intermittently occupied by steam (cf. Kokelaar 1983). This possibility is favoured by the abundant clasts of sediment, which indicate that fragmentation continued to take place at the lake floor or below. To breach the water surface these tephra jets would have had to have been much more vigorous than those producing the M1 beds, yet their limited distribution suggests a more local

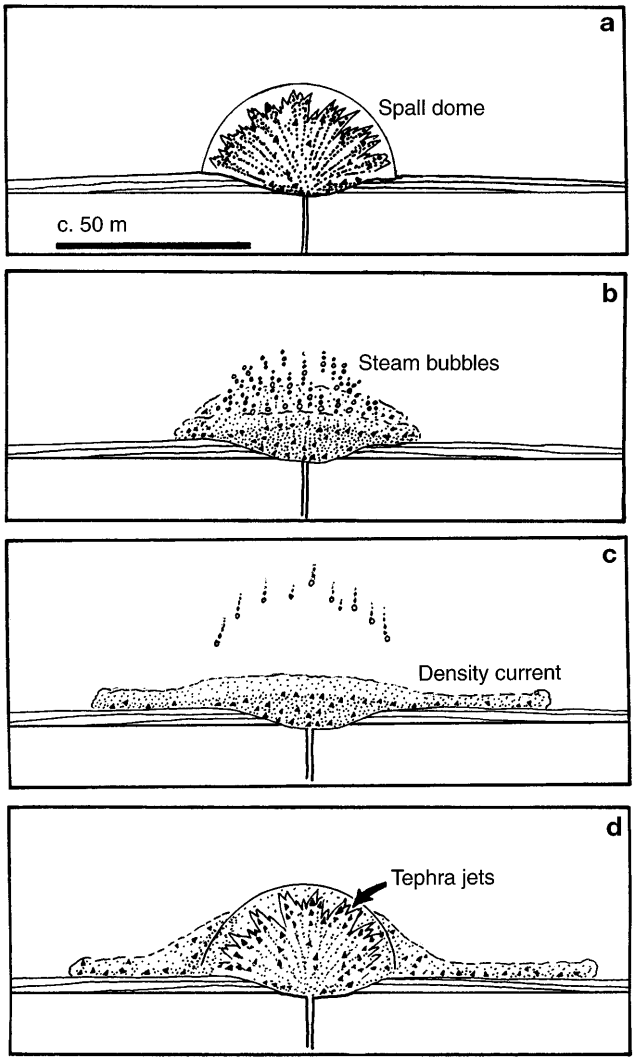

Fig. 9a–d Illustration of subaqueous jetting activity responsible for formation of facies M1 and M2. **a** Initial steamy tephra jets advance within accompanying subspherical spall dome generated by phreatomagmatic explosion(s). **b** Bubbles rise from collapsed spall dome, and tephra jets condense to release tephra particles into water column. **c** Tephra particles settle, entraining water and forming laterally flowing sediment gravity flows. **d** Succeeding eruptive pulse generates new tephra jet and spall dome, re-ejects material from vent and propels the sediment gravity flow away from the vent. Pressure waves are also associated with each explosion, passing through the surroundings well beyond the limits of the spall dome. The size of a spall dome and energy of tephra jets is dependent on explosion magnitude and water depth. For the Pahvant Butte eruption, most explosions probably produced domes up to a few tens of meters radius

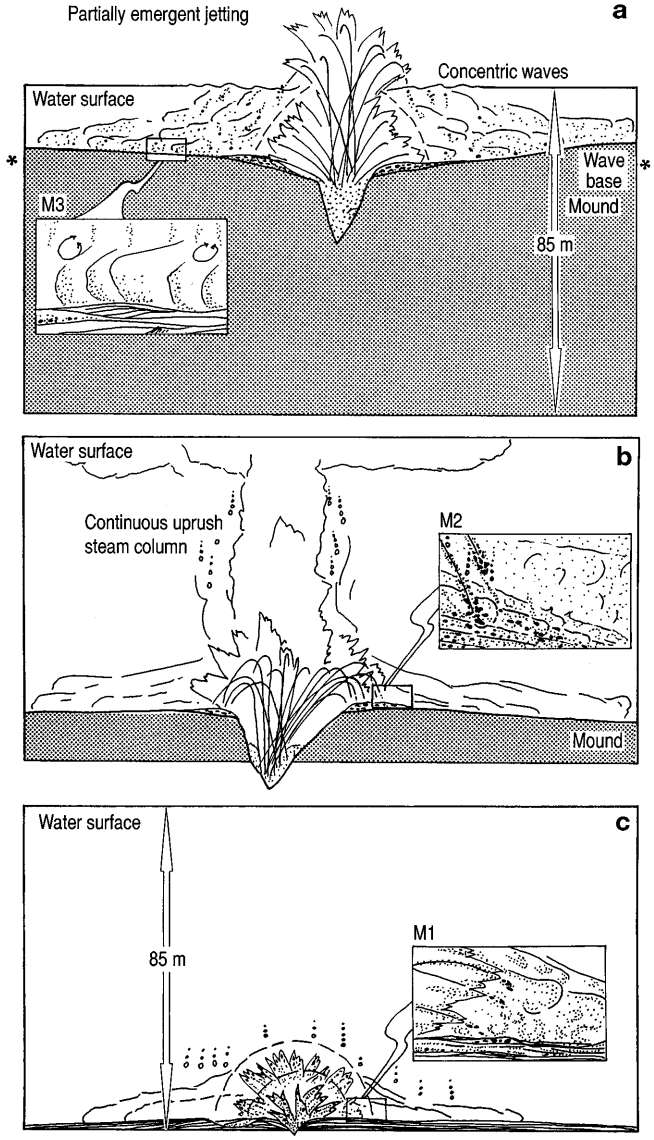

Fig. 10a–c Diagram illustrating mound growth at Pahvant Butte. Top and bottom of each frame represent lake surface and lake floor. **a** Early, fully subaqueous M1 jetting activity. Explosions and collapsing jets produce a turbulent, dilute gravity flow having strong temperature contrasts and moving unsteadily outward from the vent. Deposition takes place largely from traction under unsteady flow conditions, but occasional ejection of the vent slurry or collapse of unusually concentrated tephra jets forms high-concentration dispersions which deposit more massive M1b beds. **b** Mound (*stipple*) is shallowing. Vigorous, more-sustained activity produces local water-exclusion zones at vent margin in which clasts are transported in part through steam. This results in deposition of armoured lapilli and tachylitic clasts having impact sags (M2). Most ejecta is not deposited at vent margins, but is carried laterally in sediment gravity flows. Abundant chunks of muddy carbonate sediment in the M2 deposits at site 4 indicate minor quarrying into the lake floor during this activity. **c** Mound has now grown into shallow water (*asterisks* denote 20 m wavebase), and lithofacies M3 is being deposited. Jets are intermittently emergent. Gravity flows carrying tephra outward along the mound surface interact with oscillatory currents beneath ambient lake surface waves and longer wavelength concentric waves induced by the eruption

phenomenon. A short-lived steam cupola, or water-exclusion zone (Kokelaar 1983), would form under higher discharge, continuous uprush conditions, with development of a subaqueous eruption column (Fig. 10b). Clots, or spurts of fragmenting magma, formed the M2b beds, the coarse grain size of which is consistent with formation as a localized phenomenon, probably at the margins of an erupting subaqueous vent.

Eruption and deposition of lithofacies M3

This lithofacies was argued above to have originated by combined flow processes involving superimposition of an oscillatory wave component on depositing aqueous density currents (Fig. 10c). The considerable paleodepths to which M3 persists indicate interaction with long-wavelength waves, either formed by the eruption or, less likely, generated by an intense and widespread storm occurring simultaneously with the eruption. The higher cone rim to the north suggests that wind-formed waves during the eruption would have had a northward sense of transport, but M3 dunes at sites 1 and 3 suggest transport outward from the cone, to the west and south, respectively. Concentric, outward-travelling surface waves were reported repeatedly from the Surtsey eruptions, and were formed by explosions both subaqueously and during emergent tephra jetting (Thorarinsson 1967). Concentric waves at Surtsey had wavelengths of many meters, longer than fair-weather oceanic waves. Similar concentric waves formed during the Pahvant Butte eruption would probably be several times the wavelength of fair-weather waves in Lake Bonneville (Sly 1994).

Eruption and deposition of lithofacies M4

This lithofacies was deposited by high-sediment-concentration flows, presumably water saturated, which occurred throughout both the mound-building and subsequent stages of Pahvant Butte's growth and sedimentary evolution. The thick M4 beds containing rotated tuff blocks in a weakly stratified matrix formed by edifice failure and resedimentation. Shifts in eruptive activity generated slumps at vent margins and along slips which displaced parts of the mound. These slumps fed M4 flows which travelled only short distances before resedimenting.

Discussion

Tuff cones are small volcanoes with wide craters and steep flanks, formed by hydrovolcanic eruptions (Fisher and Schmincke 1984). Pahvant Butte and Surtsey are each frequently described tuff cones known to have formed by eruptions initiated within bodies of water (Gilbert 1890; Thorarinsson et al. 1964; Thorarinsson 1967; Condie and Barsky 1972; Kokelaar 1983; Wohletz and Sheridan 1983; Oviatt and Nash 1989; Farrand and Singer 1991, 1992), but the information concerning subaqueous eruptive activity of the two volcanoes is complementary with only minor overlap. At Surtsey eruptive processes were observed from the surface, but the subaqueous deposits resulting from it remain virtually unstudied. In contrast, Pahvant Butte offers a glimpse of the deposits inferred to have formed as the volcano grew subaqueously.

Deep-lacustrine tuff cones are "Surtseyan"

The interpretation that the Pahvant Butte eruption was "Surtseyan", or emergent, differs from recent interpretations in which initial deposition from "pyroclastic surge" was inferred to have formed M3 beds (Wohletz and Sheridan 1983; Farrand and Singer 1992). Wohletz and Sheridan (1983) inferred that the Pahvant Butte eruption began with explosive, optimal water–magma ratio explosions which generated (subaqueous?) highly inflated (with steam) pyroclastic surges, and incorporated this initial stage into their general model of tuff cones formed in lakes (Wohletz and Heiken 1992).

Lithofacies M3 formed subaqueously

The broad dunes and cross-stratification typical of M3 are at the centre of this disagreement. Vaguely similar bedforms are not uncommon in subaerially deposited pyroclastic surge beds (Crowe and Fisher 1973; Sohn and Chough 1989), but there are several reasons to discount such an origin for these beds. The most important is that this lithofacies is present *only* at altitudes below the syneruptive shoreline at Pahvant Butte, and bedding invariably has much shallower dips than any beds of the cone. It is exposed as far as 50 m below syneruptive shoreline, and grades downward into M1 beds. In addition, M3 locally has high-angle cross-stratification and ripples advancing along the gentle lee slopes of dunes, features rare in pyroclastic surge deposits but common in fluvial and marine sediments (Leeder 1982). Because M3 beds are present through much of the thickness of the mound and in association with all other lithofacies, they cannot be interpreted as subaerial deposits unless the whole of the mound formed subaerially. Sharply bounded fine-ash beds, prominent bomb sags, and other indicators of subaerial deposition, are present only in the overlying subaerial deposits of the Pahvant Butte cone (J. D. L. White, unpublished data). The distinctive stoss-depositional dunes and climbing dunes often deposited by base surges in subaerial settings are absent (e.g. Fisher and Schmincke 1984; Cas and Wright 1987; McPhie et al. 1993). Also, the coarse particle size, local high-angle cross-stratification, absence of sags and fine ash beds, and paucity of debris quarried from the substrate are all dissimilar to typical tuff ring features (e.g. Fisher and Schmincke 1984; Heiken and Wohletz 1986). Thus, despite the general similarity of bedforms with some pyroclastic surge deposits, the thick low-relief Pahvant Butte mound differs substantially from typical basaltic tuff cone or tuff ring deposits.

Surtseyan eruption and deposition of the Pahvant Butte mound

Pahvant Butte was formed by an eruption during which subaqueous tephra jetting fed relatively dilute sediment

gravity flows which distributed and deposited the bulk of tephra to form a broad subaqueous mound. The isolated appearances of M2 strata at Pahvant Butte reflect the shifting of vents during mound development. Vent structures are not well exposed, but inactive vents would have been filled by tephra from their successors and inward collapse of unstable vent walls. There was an upward transition from sub to supra-wavebase deposition as the mound grew upward from the lake floor (Figs. 3 and 4). Continuing eruption following shoaling of the mound produced largely subaerial, overlapping tuff cone strata. Littoral sediment transport and redeposition extended the platform surface over the edges of the mound. Later changes in lake level cut notches at the platform edge (Fig. 4), which were subsequently reburied when lake level rose again (J. D. L. White, unpublished data).

Tephra jetting and continuous uprush

The predominance of sediment-gravity-flow deposits over subaqueous fallout beds at Pahvant Butte is the result of a jetting-dominated eruptive style. Whereas continuous uprush produces a relatively steady column feeding a plume beneath which disseminated fallout from suspension occurs (Cashman and Fiske 1991), tephra jets return tephra to the water's surface in bursts. Delivery of a load of jetted tephra to the water allows the falling tephra mass to entrain water, forming a vertical sediment gravity flow (Allen 1982). As these flows encounter the lake floor they spread and flow laterally. This behaviour contrasts with suspension fallout, in which widely spaced particles fall through the water independently. Observations show that tephra jets are important in many emergent explosive eruptions (Thorarinsson et al. 1964; Waters and Fisher 1971), and that the process of emergence may be repeated many times during evolution of a single shoaling volcano (Hoffmeister et al. 1929; Thorarinsson 1967), together suggesting that eruption-generated aqueous sediment gravity flows are likely to be an important "Surtseyan" process. This is true as well for fully subaqueous growth, insofar as jetting activity injects discrete pulses of sediment into the water column thereby inducing behaviour quite different from the steam cupolas. The latter produce steam-insulated and high particle concentration flows, and are inferred to result from more sustained eruptive cycles (Kokelaar 1983; 1986; Mueller and White 1992).

Analogous Surtseyan deposits

Lithofacies association M1 represents fully subaqueous eruptive activity and analogous deposits are likely present at other Surtseyan volcanoes. A number of apparently Surtseyan volcanic deposits are exposed along the coastline of Otago, New Zealand, and Cas and others (1989) have described "bedded lapilli tuffs and lapillistones" from the Bridge Point locality and interpreted them as subaqueous fallout deposits. Palagonitization has made details of the Bridge Point depositional features difficult to discern (personal observation), but they show similar subtle wavy stratification, shallow scouring and variable grading characteristics to M1 beds. Further north along the coast at Cape Wanbrow, there are beds showing stronger cross-stratification, possibly analogous to M3 beds. As at Pahvant Butte, these have been interpreted as products of (subaqueous?) pyroclastic surge (Coombs et al. 1986), but unlike Pahvant Butte the original volcanic edifice has been destroyed and there has been no estimation of the depth relative to sea level at which the Cape Wanbrow deposits might have formed.

Acknowledgements This is the first instalment of a study of lacustrine volcanism supported by NSF grant EAR-91–05456 to R. V. Fisher, who helped shape the project and shared in the initial fieldwork at Pahvant Butte. Stephanie Petralia and Doris Maicher assisted with fieldwork on the Pahvant Butte mound. Reviews by J. McPhie, J. Smellie, Y. K. Sohn and S. Bull helped strengthen the manuscript significantly.

References

Allen JRL (1982) Sedimentary structures, their character and physical basis, vol 1. Elsevier, New York

Ballance PF, Tappin DR (1993) Eruption-driven gravity-flow deposition in moderate water depths on the Tonga frontal-arc platform (Miocene). Int Assoc Volcanology and Chemistry of the Earth's Interior, General Assembly, Canberra, Australia, p 5

Cas RAF, Landis CA (1987) A debris-flow deposit with multiple plug-flow channels and associated side accretion deposits. Sedimentology 34:901–910

Cas RAF, Wright JV (1987) Volcanic successions: modern and ancient. Allen and Unwin, London

Cas RAF, Landis CA, Fordyce RE (1989) A monogenetic, Surtla-type, Surtseyan volcano from the Eocene-Oligocene Waiareka-Deborah volcanics, Otago, New Zealand: a model. Bull Volcanol 51:281–298

Cashman KV, Fiske RS (1991) Fallout of pyroclastic debris from submarine volcanic eruptions. Science 253:275–280

Condie KC, Barsky CK (1972) Origin of Quaternary basalts from the Black Rock Desert region, Utah. Geol Soc Am Bull 83:333–352

Cook MA (1958) The science of high explosives. Reinhold Publishing Corporation American Chemical Society Monograph Series, New York, 440 pp

Coombs DS, Cas RAF, Kawachi Y, Landis CA, McDonough WF, Reay A (1986) Cenozoic volcanism in north, east and central Otago. In: Smith IEM (eds) Cenozoic volcanism in New Zealand. R Soc NZ Bull 23:278–312

Crowe BM, Fisher RV (1973) Sedimentary structures in base-surge deposits with special reference to cross-bedding, Ubehebe Craters, Death Valley, California. Geol Soc Am Bull 84:663–682

Dimroth E, Yamagishi H (1987) Criteria for recognition of ancient subaqueous pyroclastic rocks. Geol Surv Hokkaido Rep 58:55–88

Farrand WH, Singer RB (1991) Spectral analysis and mapping of palagonite tuffs of Pavant Butte, Millard County, Utah. Geophys Res Lett 18:2237–2240

Farrand WH, Singer RB (1992) Alteration of hydrovolcanic basaltic ash: observations with visible and near-infrared spectrometry. J Geophys Res 97:17393–17408
Fenton MW, Wilson CJL (1985) Shallow-water turbidites: an example from the Mallacoota beds, Australia. Sediment Geol 45:231–260
Fisher RV, Schmincke H-U (1984) Pyroclastic rocks. Springer, Berlin Heidelberg New York
Gilbert GK (1890) Lake Bonneville. US Geol Surv Monogr 1:1–438
Godcheaux MM, Bonnichsen B, Jenks JD (1992) Types of phreatomagmatic volcanoes in the western Snake River plain, Idaho, USA. J Volcanol Geotherm Res 52:1–25
Heiken GH, Wohletz KH (1986) Volcanic ash. University of California Press, Berkeley
Henrych J (1979) The dynamics of explosion and its use. Developments in Civil Engineering, vol 1. Elsevier, New York
Hiscott RN (1994) Loss of capacity, not competence, as the fundamental process governing deposition from turbidity currents. J Sediment Res A64:209–214
Hoffmeister JE, Ladd HS, Alling HL (1929) Falcon Island. Am J Sci 18:461–471
Houghton BF, Wilson CJN (1989) A vesicularity index for pyroclastic deposits. Bull Volcanol 51:451–462
Kneller BC, Branney MJ (1995) Sustained high-density turbidity currents and the deposition of thick massive sands. Sedimentology 42:607–616
Kokelaar BP (1983) The mechanism of Surtseyan volcanism. J Geol Soc Lond 140:939–944
Kokelaar BP (1986) Magma–water interactions in subaqueous and emergent basaltic volcanism. Bull Volcanol 48:275–289
Kokelaar BP, Durant GP (1983) The submarine eruption and erosion of Surtla (Surtsey), Iceland. J Volcanol Geotherm Res 19:239–246
Leeder MR (1982) Sedimentology, process and product. Allen and Unwin, London
Lowe DR (1982) Sediment gravity flows. II. Depositional models with special reference to the deposits of high-density turbidity currents. J Sediment Petrol 52:279–297
Lowe DR (1988) Suspended-load fallout rate as an independent variable in the analysis of current structures. Sedimentology 35:765–776
McPhie J, Doyle M, Allen R (1993) Volcanic textures: a guide to the interpretation of textures in volcanic rocks. CODES Key Centre, University of Tasmania Hobart
Mueller W, White JDL (1992) Felsic fire-fountaining beneath Archean seas: pyroclastic deposits of the 2730 MA Hunter Mine Group, Quebec, Canada. J Volcanol Geotherm Res 54:117–134
Oehmig R (1993) Entrainment of planktonic foraminifera: effect of bulk density. Sedimentology 40:869–877
Oviatt CG, Nash WP (1989) Late Pleistocene basaltic ash and volcanic eruptions in the Bonneville basin, Utah. Geol Soc Am Bull 101:292–303
Postma G, Roep TB, Ruegg GHJ (1983) Sandy–gravelly mass-flow deposits in an ice-marginal lake (Saalian, Leuvenumsche Beek Valley, Veluwe, The Netherlands), with emphasis on plug-flow deposits. Sediment Geol 34:59–82
Raaf JFM de, Boersma JR, Gelder A van (1977) Wave-generated structures and sequences from a shallow marine succession, Lower Carboniferous, County Cork, Ireland. Sedimentology 24:451–483
Schmid R (1981) Descriptive nomenclature and classification of pyroclastic deposits and fragments: recommendations of the IUGS Subcomission on the Systematics of Igneous Rocks. Geology 9:41–43
Sly PG (1994) Sedimentary processes in lakes. In: Pye K (ed) Sediment transport and depositional processes. Blackwell, Oxford, pp 157–192
Sohn YK, Chough SK (1989) Depositional processes of the Suwolbong tuff ring, Cheju Island (Korea). Sedimentology 36:837–855
Sohn YK, Chough SK (1992) The Ilchulbong tuff cone, Cheju Island, South Korea: depositional processes and evolution of an emergent, Surtseyan-type tuff cone. Sedimentology 39:523–544
Southard JB (1991) Experimental determination of bed-form stability. Annu Rev Earth Planet Sci 19:423–455
Staudigel H, Schmincke H-U (1984) The Pliocene seamount series of La Palma/Canary Islands. J Geophys Res 89:11195–11215
Thorarinsson S (1967) Surtsey. The New Island in the North Atlantic. Viking Press, New York
Thorarinsson S, Einarsson T, Tigvaldason GE, Elisson G (1964) The submarine eruption off the Westmann Islands 1963–1964. Bull Volcanol 27:1–11
Waters AC, Fisher RV (1971) Base surges and their deposits: Capelinhos and Taal volcanoes. J Geophys Res 76:5596–5614
White JDL, Busby-Spera CJ (1987) Deep marine arc apron deposits and syndepositional magmatism in the Alisitos group at Punta Cono, Baja California, Mexico. Sedimentology 34:911–928
White JDL, Fisher RV (1993) The growth and sedimentary evolution of a volcano erupted into Lake Bonneville, Utah. Int Assoc Volcanology and Chemistry of the Earth's Interior, General Assembly, Canberra, Australia, p. 121
Wohletz K, Heiken G (1992) Volcanology and geothermal energy. University of California Press, Los Alamos Series in Basic and Applied Sciences, Berkeley, 432 pp
Wohletz KH, Sheridan MF (1983) Hydrovolcanic explosions II. Evolution of basaltic tuff rings and tuff cones. Am J Sci 283:384–413
Yamamoto T, Soya T, Suto S, Uto K, Takada A, Sakaguchi K, Ono K (1991) The 1989 submarine eruption off eastern Izu Peninsula, Japan: ejecta and eruption mechanisms. Bull Volcanol 53:301–308